

Feedback from galactic stellar bulges and hot gaseous haloes of galaxies

Shikui Tang, Q. Daniel Wang, Yu Lu, and H. J. Mo

Department of Astronomy, University of Massachusetts, 710 North Pleasant Street, Amherst, MA 01003

ABSTRACT

We demonstrate that the feedback from stellar bulges can play an essential role in shaping the halo gas of galaxies with substantial bulge components by conducting 1-D hydrodynamical simulations. The feedback model we consider consists of two distinct phases: 1) an early starburst during the bulge formation and 2) a subsequent long-lasting mass and energy injection from stellar winds of low-mass stars and Type Ia SNe. An energetic outward blastwave is initiated by the starburst and is maintained and enhanced by the long-lasting stellar feedback. For a Milky Way-like galactic bulge, this blastwave sweeps up the halo gas in the proto-galaxy and heats up the surrounding medium to a scale much beyond the virial radius of the halo, thus the accretion of the halo hot gas can be completely stopped. In addition to that, the long-lasting feedback in the later phase powers a galactic bulge wind that is reverse-shocked at a large radius in the presence of surrounding intergalactic medium and hence maintains a hot gaseous halo. As the mass and energy injection decreases with time, the feedback evolves to a subsonic and quasi-stable outflow, which is enough to prevent halo gas from cooling. The two phases of the feedback thus re-enforce each-other's impact on the gas dynamics. The simulation results demonstrate that the stellar bulge feedback may provide a plausible solution to the long-standing problems in understanding the Milky-Way type galaxies, such as the “missing stellar feedback” problem and the “over-cooling” problem. The central point of the present model is that the conspiracy of the two-phase feedback keeps a low density and a high temperature for the halo gas so that the X-ray emission from the diffuse gas is significantly lowered and the radiative cooling is largely suppressed. The simulations also show that the properties of the hot gas in the subsonic outflow state depend sensitively on the environment and the formation history of the bulge. This dependence and variance may explain the large dispersion in the X-ray to B-band luminosity ratio of the low L_X/L_B elliptical galaxies.

Subject headings: galaxies: bulges — galaxies: ISM — ISM: evolution — ISM: structure — intergalactic medium — X-rays: ISM

1. INTRODUCTION

It is believed that galaxies form in dark matter halos, which grow through gravitational instability from the density fluctuations seeded in the early universe. The baryonic matter is then accreted into the dark matter halos and cools radiatively to assemble galaxies. Although the structure and the evolution of dark matter halos are fairly well understood with the use of analytic modeling (Press & Schechter 1974; Bond et al. 1991; Sheth et al. 2001) and N -body simulations (Navarro, Frenk & White 1996; Jing & Suto 2000; Moore et al. 1998), galaxy formation still remains a challenging problem as it is a complex process involving simultaneous actions of many physical mechanisms.

One of the long-standing problems in galaxy formation is that, in the absence of heating sources, the majority of baryons in the Universe is predicted to have cooled into dark matter halos by the present time (e.g. White & Rees 1978; White & Frenk 1991), while in reality only a small fraction of the baryons associated with galaxies is observed in the cold (stars plus cold gas) phase (Maller & Bullock 2004; Mo et al. 2005; Fukugita & Peebles 2006; Sommer-Larsen 2006). This “over-cooling” problem implies that feedback must have played a very important role in shaping galaxies. A number of feedback mechanisms have been proposed, each of which works only for a limited range of halo mass scales. For example, the heating by the UV background is expected to be effective only in small halos with masses $M < 10^{10} M_\odot$ at low redshift (Quinn et al. 1996; Gnedin 2000; Hoeft et al. 2006). The supernova (SN) feedback from instantaneous star formation may blow out gas from dwarf galaxies with halo mass less than $10^{11} M_\odot$ but become much less effective in massive halos (MacLow & Ferrara 1999). AGN feedback powered by the central massive black holes works efficiently only for halos more massive than $10^{13} M_\odot$ (e.g. Wyithe & Loeb 2003; Croton et al. 2006; Lu & Mo 2007). It turns out to be the most difficult to solve the “over-cooling” problem in Milky-Way sized halos (with masses $\sim 10^{12} M_\odot$), presumably because here various feedback processes, such as the pre-heating of the IGM, the supernova explosions and the active galactic nuclei (AGNs) (e.g., Mo & Mao 2002; Toft et al. 2002; Davé & Oppenheimer 2007), can all play some role in affecting the gas accretion and star formation.

Energetically, the ongoing galactic feedback appears to be sufficient to balance the cooling. Indeed, much of the expected mechanical energy from supernovae (SNe) feedback is “missing” at least from X-ray observations (David et al. 2006; Li et al. 2006, 2007; Li & Wang 2007). In general, the observed X-ray emission consists of several components: 1) relatively bright X-ray binaries with neutron star and black hole companions ($\sim 10^{36} - 10^{38}$ ergs s $^{-1}$), which may be detected individually in nearby galaxies; 2) numerous cataclysmic variables (CVs) and coronally active binaries (ABs) ($\sim 10^{30} - 10^{33}$ ergs s $^{-1}$), which are too faint to be detected individually, but can be constrained based on near-IR emission (Revnivtsev et al. 2006; Li et al. 2007); 3) diffuse hot gas heated chiefly by Type Ia SNe. The typical observed diffuse X-ray emission only accounts for a few percent of the expected SN energy input (e.g., Li et al. 2007; Li & Wang 2007), the majority of which is undetected. This missing feedback problem becomes particularly acute in the low L_X/L_B bulge-dominated galaxies (typically Sa spirals, S0, and low mass ellipticals), in which the presence

of little cool gas can hardly hide or radiate the energy in other wavelength bands. Naturally, one would expect that the missing energy in such galaxies is gone with a galactic outflow, which could have a profound impact on the halo gas and the accretion of the IGM. Of course, this impact should evolve with time and depend on the formation process of the galaxy. For example, if a bulge forms primarily in a starburst (SB), it can induce an initial blastwave propagating into the surrounding medium. The heated environmental medium can then affect the impact of the later feedback from stellar mass loss and Type Ia supernovae (SNe) as well as from star formation. Therefore, one needs to study the interplay of the stellar feedback and the gas accretion of the galaxies to understand their evolution.

Existing studies have shown the importance of the stellar feedback, though they are limited by the over-simplified treatments or are for some specific targets. On the one hand, existing models for galactic bulge outflows/winds include little consideration for the evolving gravitational potential and gaseous environment (e.g., Mathew & Baker 1971; White & Chevalier 1983; Lowenstein & Mathews 1987; Ciotti et al. 1991; David et al. 1991; Pellegrini & Ciotti 1998). On the other hand, in simulations of large-scale structure formation, the treatment of the stellar feedback is limited by the spatial resolution. A more sophisticated model that incorporates the stellar feedback in an evolving galaxy has been investigated by Brighenti & Mathews (1999) with 1-D hydrodynamic simulation. They found that the core-collapse SNe in an initial SB can substantially affect the gas dynamics beyond 1 Mpc. But the work was done specifically to explain the hot gaseous properties of the luminous elliptical galaxy NGC 4472. In this high-mass galaxy, later feedback is found to be unimportant, partly because the author adopted a low SN rate (0.03 SNu; one SNu unit denotes one SN per $10^{10} L_{B\odot}$ per century). In this case, the gas dynamics is dominated by a cooling flow.

In the present paper, we introduce a stellar feedback model in which the feedback is closely associated with the formation history of the galactic bulges. In this scenario, we divide the evolution of a bulge into three stages: 1). At high redshift, as the host dark matter halo assembles, the central galaxy builds up a bulge through frequent major mergers. 2). As a consequence of the violent mergers, a SB in the bulge is triggered. The intensive starburst powers a blastwave to sweep up the halo gas and to prevent the new gas from infalling into the halo. 3). At low redshift, the galaxy is in a quiescent phase as its host halo accretes mass gently. However, as the low-mass bulge stars die off from the main sequence, Type Ia SNe provide a long-lasting energy input to the intergalactic medium (IGM) and this gradual feedback maintains a hot gaseous halo. This scenario naturally connects the stellar feedback and the general formation history of a galaxy. We find that such a feedback can profoundly affect the evolution of the model galaxies. In particular, the overcooling and missing-energy problems can be naturally explained. Here we demonstrate the effects of the feedback based on a 1-D model of galaxies, although limited 2- and 3-D simulations have also been carried out to check multi-dimensional effects. Our aim here is to capture qualitatively the feedback effects on the structure, physical state, and dynamics of the hot gas around bulge-dominated galaxies on scales greater than galactic bulges/disks.

The organization of the paper is as follows. We first describe the main physical ingredients of our model and numerical methods (§2). We then present the results of a reference galaxy model and its variations (§3). In §4, we discuss how the results provide a potential solution to the overcooling and missing energy problems, as well as the caveats of the present model. We summarize our results and conclusions in §5.

2. Galaxy Model and Methodology

We set up hydrodynamical simulation models to investigate the effects of the feedback from a galactic stellar bulge on galaxy formation. We focus our study on the early-type spirals and/or the typical low - L_X/L_B elliptical galaxies in fields or in small groups (such as the MW and M31). These galaxies have an intermediate/massive galactic bulge and have dark matter halos with masses $\sim 10^{12} M_\odot$ at the present time. In the following, we first describe how such a galaxy assembles mass during the buildup of the gravity potential of the growing dark matter halo. We then introduce the recipe to model the stellar bulge formation and its feedbacks. Finally we describe the numerical codes and methods used to explore the stellar feedback on the gas dynamics. Throughout the paper, we adopt the Λ CDM cosmology with $\Omega_m = 0.3$, $\Omega_\Lambda = 0.7$ and $H_0 = 100 \text{ km/s/Mpc}$. We assume the universal cosmic baryon fraction to be $f_b = 0.17$.

2.1. The Growth of Dark Matter Halo

It has been shown by high resolution N -body simulations that within the virial radius r_{vir} the density profile of a collapsed dark matter halo can be well described by the NFW profile (Navarro, Frenk & White 1996),

$$\rho_{\text{NFW}}(r) = \frac{4\rho_0}{(r/r_s)(1 + r/r_s)^2}, \quad (1)$$

where r_s is a characteristic radius and ρ_0 a characteristic density of the halo that is related to the collapse time of the halo. The shape of such a profile is usually characterized by the concentration parameter, defined as $c = r_{\text{vir}}/r_s$. Since a virialized halo is defined as a spherical region with a mean density that is Δ_{vir} times the mean density of the Universe, the characteristic density can be written as

$$\rho_0 = \frac{1}{12} \rho_{\text{crit}} \Omega_m \Delta_{\text{vir}} \frac{c^3}{\ln(1+c) - c/(1+c)}, \quad (2)$$

where ρ_{crit} is the critical density of the Universe. For the cosmology we adopted here, $\Delta_{\text{vir}} = 340$ at $z = 0$ (Bryan & Norman 1998). For a given cosmology, a virial mass, and a given time, the density profile of a dark matter halo is determined by the single parameter, c . Simulations of the formation of dark matter halos have demonstrated that dark matter halos assemble their mass through an early fast accretion phase followed by a slow accretion phase (Wechsler et al. 2002;

Zhao et al. 2003a). This two-phase assembly history can be fairly well described by an exponential function (Wechsler et al. 2002),

$$M(a) = M_0 e^{-2a_c(\frac{1}{a}-1)}, \quad (3)$$

where M_0 is the halo mass at the present time, a is the expansion scale factor [i.e., $a = (1+z)^{-1}$, z is the redshift], and a_c is the scale factor at the halo ‘formation time’ that separates the two accretion phases. Both N -body simulations (Bullock et al. 2001; Wechsler et al. 2002; Zhao et al. 2003a,b) and analytical model (Lu et al. 2006) have shown that the halo concentration parameter is closely related to the formation time a_c . For a halo that is still in its fast accretion regime, $c \sim 4$; for a halo identified at $a > a_c$, $c \sim 4a/a_c$. To reproduce the evolution of the mass distribution of a forming dark matter halo, we make use of the 1-D simulation code developed by Lu et al. (2006) to simulate the growing dark halo embedded in the cosmic density field. Following Lu et al. (2006) and Lu & Mo (2007), we setup the initial perturbation at $z_i = 100$. The perturbation profile is set up in such a way that the subsequent accretion history of the halo follows exactly the average mass accretion history given by Eq.(3). The halo’s virial mass is $10^{12} M_\odot$ at the present time. To be consistent with the statistical properties of dark halos in cosmological simulations, we choose the formation time $a_c = 0.3$. The resulting halo has a concentration of about 13, which is typical for halos of such a mass. The advantage of adopting this approach is that, at any redshift, the density profiles both within and outside the current virial radius are modeled realistically. Fig. 1 shows the density profiles of the simulated halo at four different redshifts. We find that the evolution of our simulated profile can be fitted with the following formula:

$$\rho(r, t) = \begin{cases} 4\rho_0 / [x(1+x)^2], & x = r/r_s \text{ for } r \leq r_v \\ \rho(r_v, t) [\frac{8}{9} (\frac{r}{r_v})^{\alpha(t)} + \frac{1}{9} (\frac{r}{r_v})^{-1}], & \text{for } r > r_v \end{cases} \quad (4)$$

where t is the cosmic time in Gyr; r_v is the halo virial radius at time t and r_s is the scale radius of the NFW profile at $z=0$; $\alpha(t) = -46 + 9.4t - 0.58t^2$ is a time-dependent index obtained from fitting the simulated profiles at $r \gtrsim r_v$. This formula (illustrated as the solid red lines in Fig. 1) characterizes the simulated profiles to an accuracy of 5% in the interested region. We adopt this fitting function in the hydro-dynamical simulations to calculate the gravity from the dark matter, so that the computational cost for the gravity is greatly reduced. Although the deposition of the cold gas in the halo center may make the the halo contract (Blumenthal et al. 1986; Choi et al. 2006), our test with the same 1-D simulation code but including the gravity of the cool gas shows that the change of the dark matter distribution is only in the central several kpc, and that our main results on the halo gas properties are not expected to be affected significantly by such contraction.

2.2. Stellar Bulge Feedbacks

We assume that the stellar bulk in our model galaxy forms in a single starburst at the time t_{sb} right after the fast-accretion regime of the dark matter halo, when the inner halo is well established and the gas cools fast compared to the halo dynamical time-scale. Dense gas clouds are thus

expected to form rapidly, leading to rapid star formation (Mo & Mao 2004). We approximate the stellar feedback into two phases: (1) a blastwave generated by the initial SB that forms the stellar bulge and (2) a gradual injection of mass and energy through stellar mass-loss and Type Ia SNe in the bulge. Additional feedback may arise from the galactic disk, if present (although cool gas there may consume much of the input energy), and from AGNs. We do not deal with these complications here, which may be incorporated into the above two phases approximately within the uncertainties in our adopted feedback parameters.

2.2.1. Starburst feedback

We parameterize the SB feedback with an estimate of the mechanical energy input from core-collapsed SNe. This estimate depends on the uncertain initial mass function (IMF) of the stars formed in the SB. Assuming the commonly used Salpeter IMF over the mass range of 0.08-100 M_\odot , for example, the number of the stars with individual masses greater than 8 M_\odot is $N_{>8} = 6.8 \times 10^{-3} M_*$; but a probably more realistic IMF with a low mass turn-over (e.g., Miller & Scalo 1997; Kroupa 2001) can give a substantially higher value. We estimate the total energy deposited into the large-scale surrounding as

$$E_{\text{SB}} = \eta E_{\text{sn}} N_{>8} = 6.81 \times 10^{-3} \eta M_* E_{\text{sn}}, \quad (5)$$

where $E_{\text{sn}} = 10^{51}$ ergs is assumed to be the energy of each SN. The parameter η characterizes the “efficiency” of the energy deposit, accounting for the uncertainties in the assumed IMF, E_{sn} , possible energy release from other sources (e.g., AGN), and the radiative dissipation within the SB region. The radiative dissipation, for example, depends on the unknown details of the interaction between the SB and the interstellar medium (ISM; e.g., its porosity; Silk 2003). Here we simply treat η as a free parameter. We do not attempt to study the evolution of the SB itself or its immediate interaction with the cold gas in the bulge (e.g., Strickland & Stevens 2000; Fujita et al 2004). As we focus on the potential impact of the SB on the ambient hot gas over much larger physical and time scales, the exact fashion of the SB (e.g., coeval vs. exponential over a time scale

Table 1. Model galaxy parameters

| Parameter | Value |
|---|--------------------|
| Halo mass M_0 (M_\odot) | 10^{12} |
| SB gas mass M_{sb} (M_\odot) | 5×10^{10} |
| Bulge stellar mass M_* (M_\odot) | 3×10^{10} |
| Bulge scale r_b (kpc) | 0.7 |
| SB time t_{sb} (Gyr) | 2.5 |
| SB energy deposit region R_{sb} (kpc) | 50 |
| Age of galactic bulge t_0 (Gyr) | 10 |

of $\sim 10^8$ yr) should make negligible difference in our simulations.

2.2.2. Gradual feedback

Following the core-collapsed SNe of massive stars ($M \gtrsim 8M_\odot$) is this long-lasting, but relatively gentle feedback from stars of lower masses. The energy input from the gradual feedback is primarily from Type Ia SNe. The average local SN Ia rate for E/S0-type galaxies is 0.12 (Cappellaro et al 1999; Arthur 1999, p467). The exact evolution of the Type Ia SN rate in each type of galaxies is largely unknown; a power law is generally adopted (e.g., Ciotti et al. 1991; Brighenti & Mathews 1999): $R_{\text{sn}}(t) = R_0(t/t_0)^{-p}$, where R_0 (in the unit of SNU) is the SN Ia rate of a stellar population at an age t_0 (Table 1). We assume that $p = 1.4$ as in Ciotti et al. (1991), and that the Type Ia SN starts 0.1 Gyr (Greggio 2005; Mannucci et al. 2006; Aubourg et al. 2007) after the starburst. Thus the energy input rate from Type Ia SNe is

$$L_{\text{SNIa}}(t) = E_{\text{sn}} \left(\frac{L_B}{10^{10}} \right) \frac{R_0}{100} \left(\frac{t}{t_0} \right)^{-p}, \quad (6)$$

where t is the age of stellar population, and L_B is the blue band luminosity of the stellar population at an age t_0 (Table 1) and can be determined based on stellar evolutionary model (e.g., Maraston 2005). Note that observationally L_B is easily biased by newly formed stars, and the K -band luminosity, L_K , may be a better proxy to trace the bulk of the old stellar population. Theoretically, however, the choices of L_B and L_K are equivalent, and the conversion from L_B to L_K is determinable (e.g., Maraston 2005). We nevertheless use L_B as the proxy and interpret Eq. (6) with caution.

The stellar mass loss is also time-dependent and related to the stellar age. Most of the stellar mass loss occurs at early time through the relatively fast evolution of intermediate-mass stars. For a stellar population with the standard Salpeter IMF, Ciotti et al. (1991) show that the mass loss rate can be described by a power law:

$$\dot{M}(t) = 1.5 \times 10^{-11} L_B t_{15}^{-1.3} \text{ M}_\odot \text{ yr}^{-1} \quad (7)$$

where L_B is the blue band luminosity of the stellar population at 15 Gyr and t_{15} is its age in the unit of 15 Gyr. The equation is valid only for $t > 0.5$ Gyr. This formula is somewhat difficult to apply based on observed L_B because L_B is easily biased by newly formed stars and the age of the bulk stellar population is quite uncertain and hard to determine. Here we use an updated calculation obtained from Maraston (2005, Fig. 22), which directly relates mass loss to the total initial mass of a stellar population. The cumulative stellar mass loss of a normalized stellar population of 1 M_\odot initially can be fitted by the following formula:

$$M(< t) = 0.798 - 0.124t^{-0.3} + 0.0748e^{-t/0.18}, \quad (8)$$

where t is the age of stellar population in the unit of Gyr. In general, the fitting formula provides an accuracy to 1% of the numerical result and is valid in the range from 0.1 Gyr to 15 Gyr. Eq. (8)

and Eq. (7) give the same shape for $t > 1$ Gyr but the conversion depends on the mass-to-light ratio M/L_B . Taking the M/L_B as about 10.3 for a stellar population at 15 Gyr (Maraston 1998), the mass loss rate given by Eq. (8) is about three-fourth of that by Eq. (7).

It is worth comparing the relative energetics of the stellar feedback during the SB and the later gradual phase. There is 6.8×10^{-3} SNe II per solar mass for a standard Salpeter IMF. For a general power law decay of the SNe Ia rate, the number of SNe Ia per solar mass is $10^{-3} R_0 (M/L_B)^{-1} n_{Ia}$, where (M/L_B) is the mass to light ratio, and n_{Ia} is the integral

$$n_{Ia} = \int_{t_{em}}^{t_{now}} \left(\frac{t}{t_0} \right)^{-p} dt, \quad (9)$$

where t_{em} is the emerging time of SNe Ia after SB, and t_{now} is the current age of the bulge. We fix t_{now} at 10 Gyr as a typical age of galactic bulges ($t_0=10$ Gyr as well). The M/L_B for a single stellar population with standard Salpeter IMF is about 7 at 10 Gyr (Maraston 1998), and n_{Ia} is nearly unaffected in a reasonable range of t_{now} . The value of n_{Ia} depends on the choice of t_{em} and p , and within a reasonable range of t_{em} (e.g, 0.1-0.5 Gyr) and p (e.g, 1.0-1.4), $n_{Ia} \simeq 100$ with an uncertainty about a factor of two. Thus the number of SNe Ia per solar mass is $\sim 1.7 \times 10^{-3} \left(\frac{R_0}{0.12} \right) \left(\frac{7}{M/L_B} \right) \left(\frac{n_{Ia}}{100} \right)$. SB feedback in principle provides much more energy in a short time than the gradual feedback does in the life time of a galactic bulge. Note that the time in Eq. (6)-(9) is based on “stellar clock” and modeled independent of cosmology, but in simulation we assume that the “stellar clock” is consistent with the concordance cosmology model (where $h = 0.7$). Hence the time unit in Eq. (6) and (8) in our simulation is scaled accordingly.

2.3. Gas Evolution Simulation

We combine two methods to simulate the gas evolution in the model galaxy. To accurately represent the accretion of the mass onto the simulated galaxy halo and the formation of the bulge in the fast assembly regime of the dark matter halo, we adopt the 1-D Lagrangian hydrodynamical code (Lu & Mo 2007). As we introduced in §2.1, the Lagrangian code simulation starts from density perturbation at $z_i = 100$. We use 1000 and 100,000 shells to represent gas and dark matter, respectively. Before the mass collapses into the virial radius the two components follow each other. When a gas shell is shocked roughly at the virial radius, the gas is decoupled from dark matter movement and is heated up to the virial temperature. The gas then cools radiatively. When the temperature falls below 2×10^4 K, the gas shell is considered to be cold and is dropped out from the hot phase. We re-distribute the dropped-out cold gas into the halo center according to the Hernquist profile (Hernquist 1990) with the scale radius of 0.7 kpc. We terminate the 1-D Lagrangian simulation at $z = 1.8$ when the fast-accretion regime is over. This simulation provides both the mass of the dropped-out gas (M_b) and the density, temperature, and velocity profiles of the remaining hot gas. The output of gas properties from the Lagrangian code is adopted as the initial condition for our feedback simulations. We resort to an Eulerian based code which is easier

to handle the position-wise mass and energy input.

After the fast assembly epoch, the bulk of the galactic bulge has been built up and the SB is triggered. In the SB a fraction (f_{SB}) of the dropped-out mass M_{b} is converted into stars (M_*). The rest cold gas remains the Hernquist distribution and contributes only the gravity to the gas dynamics in the subsequent evolution. We deposit the mass and energy of the SB feedback uniformly in an inner region of radius $R_{\text{sb}} = 50$ kpc, which is about the virial radius of the halo at the assumed SB epoch (Table 1). The included gas is assumed to be well mixed with the ejecta of the SNe and is thus considered to be SB-enriched. We have experimented various methods to deposit the SB energy (e.g., kinetic vs. thermal energy as well as radius) and find that they don’t make significant differences as long as no additional dissipation is allowed before the deposited energy emerges into the large-scale surrounding.

With the feedback included, we conduct our hydrodynamical simulations using the widely-used FLASH code (Fryxell et al 2000). It is a modular, adaptive-mesh, Eulerian based hydrodynamic code capable of handling general compressible flow problems. The hydrodynamic solver we adopted is a directionally split piecewise-parabolic method (PPM) which is formally accurate to second order in both space and time (see also FLASH User’s Manual). The gravity force includes the dark matter halo with a time-dependent density profile described by Eq. (4) and a fixed Hernquist profile for the stellar bulge with a total mass of M_{sb} (Table 1). This approximation of the gravity force does not account for both the stellar mass loss and the deviation of the cold gas mass distribution from the assumed profile (e.g., the cold gas may reside primarily in a disk or could have been reheated later). The gas self-gravity is also ignored in the gas dynamics simulations. The effect of these complications should be small on the gravity, which is dominated by the bulge stellar mass at small radii and by dark matter at large radii. The mass and energy input, specified by Eq. (6) and (8), follow the stellar mass distribution. The source terms are handled by the operator split method in FLASH.

The radiative cooling of the gas depends on its metallicity as well as its local density and temperature in the simulations. We assign representative metallicities of 0.01, 0.1, and 1 solar to the IGM, the SB-enriched gas, and the Type Ia SN-enriched stellar material. A 0.1 solar abundance of the SB-enriched gas corresponds to roughly a yield of $0.02 M_{\odot}$ metals per solar mass of the SB. The metallicity-dependent cooling function is adopted from Sutherland & Dopita (1993). Radiative cooling is switched off for gas of the temperature below 2×10^4 K, which could be maintained by the extra-galactic UV/X-ray background heating. The different metallicities are also used to track the individual gas components.

In our investigation we focus on the stellar feedback on an MW-like galaxy. We assume that the SB converts a fraction ($f_{\text{SB}} \simeq 0.6$) of the cooled bulge mass M_{b} into stars (M_*), which gives the bulge mass comparable to the MW bulge. The adopted values are listed in Table 1. We have chosen a set of models to investigate how the dynamics and observational properties of the hot gas depend on the SB strength, the variations of gradual stellar feedback, and the treatment of cold

gas. The model parameters are summarized in Table 2. The fiducial model (Model Ref.) adopts the canonical values, which sets the reference for other model variations. We demonstrate the effects of the SB strength in Model VA, the varied mass loading in Model VB, and the varied Type Ia SN feedback in Model VC and VD. The effect of cooled gas on the gas dynamics is examined in model VE.

Our simulation radius is 2 Mpc around a model galaxy, including all the region that the feedback can influence. Because gas at this radius is still participating in the Hubble expansion, an “outflow” (zero-gradient) boundary condition is adopted, while the standard “reflection” boundary condition is used at the center.

3. Results

In this section, we first focus on the fiducial model and then change some of the important model parameters to see the resultant variance in the dynamics of the hot halo gas. We then show the immediate predictions of our model on the halo gas fraction and X-ray brightness.

3.1. Dynamical Structures and Evolution

3.1.1. Reference Model

Fig. 3 illustrates the gas properties of the reference model galaxy at three representative redshifts. Soon after the SB (e.g., $z=1.4$; dot-dashed line), a blastwave (corresponding to the jump at $r \sim 10^{2.5}$ kpc in all the four panels) is driven into the accretion flow of the galaxy. This accretion flow is most apparent in the radial velocity panel (i.e., the negative velocity just in front of the blastwave). At larger radii, the gas is still trailing the Hubble expansion. Later, the blastwave, though weakening, catches up the trailing gas (i.e., no negative velocity at $z = 0.5$ and 0.0). The blastwave heats the gas to a temperature of $\gtrsim 10^6$ K, over a region extending well beyond the virial radius at $z \sim 1.4$ (~ 80 kpc) and even at $z = 0.0$ (~ 200 kpc). Consequently, *after this pre-heating by the SB-induced blastwave, no virial shock forms.*

The SB heating also allows for the transportation of the later stellar feedback away from the galactic bulge. Without the SB heating and the resultant rarefaction of the surrounding gas, the energy from the Type Ia SNe would be radiated away around the bulge and the gradual feedback could never launch a galactic bulge wind. With the low density of the ambient gas due to the expansion, the gradual stellar feedback develops into a galactic bulge wind, at least in early time when the SN rate is high. This wind reaches a velocity up to $\sim 10^3$ km s $^{-1}$ at $z = 1.4$ and ~ 800 km s $^{-1}$ at $z = 0.0$ as the rate decreases. The wind is reverse-shocked at a quite large radius (the inner most jumps of the profiles in Fig. 3). The reverse-shock first moves outward and then starts to move back toward the center as the Type Ia SN rate declines with time. The

reverse-shocked wind material has a temperature of $\sim 10^7$ K. This temperature is determined by the specific energy of the feedback, minus the potential that the wind needs to climb through. The radiative cooling of the wind is negligible (see Table 2 and later discussion in §4.2). Therefore, the SB heating enables the impact of the Type Ia SN-driven feedback over global scales around the galaxy.

In return, the long-lasting Type Ia SN-driven feedback helps to maintain and even to enhance the low-density hot environment produced by the SB. First, the inauguration of the Type Ia SN-driven feedback about 0.1 Gyr after the SB generates a forward shock, which can be seen in Figure 3 (bottom panel) as a small velocity jump just behind the SB blastwave. This shock propagates fast in the SB-heated gas with little radiative energy loss (Tang & Wang 2005) and quickly overtakes the SB blastwave. Secondly, the Type Ia SN-driven stellar feedback prevents the SB-heated gas from falling back toward the galactic center to form a cooling flow, which would generate too large an X-ray luminosity to be consistent with observations.

Sandwiched between the shocked bulge-wind material and the blastwave-heated IGM is the SB-enriched gas (e.g., marked as the gray region for the $z = 1.4$ density profile). The two contact-discontinuities around the gas are apparent in the density and temperature profiles of Fig. 3. The SB-enriched gas has a relatively high density and a low temperature; and the gas has a cooling time scale of ~ 1 Gyr even with the assumed moderate metallicity. The gas can cool to the lowest temperature allowed (2×10^4 K in our simulation) first, as represented by spike-like features in the density profiles at lower redshifts. This collapsed dense shell is subject to various hydrodynamical instabilities (if not prevented by the presence of magnetic field); the fragmented cool gas may be decoupled from the hot gas flow.

3.1.2. Dependence on the SB feedback efficiency

The most uncertain parameter in our reference model is η , which determines the magnitude of the SB energy feedback. In Model VA we reduce the SB feedback efficiency to $\eta = 0.25$. The results are compared with those from the reference model in Fig. 4 at $z = 0$. Naturally, a smaller η value gives a slower and weaker SB blastwave, hence a relatively higher density and faster cooling of the interior gas. The velocity becomes negative around virial radius and the material blown away earlier is being re-accreted into the halo.

This relatively high density halo environment affects the dynamics of the Type Ia SN-driven feedback, which is confined to a smaller region (Fig. 4). An interesting feature of this model is the higher temperature of the reverse shocked bulge wind material, which has not lost much of its energy in climbing out the gravitational potential of the galaxy. The noticeable wiggles in the profiles of temperature and density are generated by the unstable cooling when the dense shell forms. The reverse shock is moving inward and is only about 20 kpc away from the center of the galaxy at $z = 0$. When it eventually reaches the center, the bulge wind will be quenched. After

that, a cooling flow of previously reverse-shocked bulge wind material will form. The cooling flow, together with the infall of the already cooled SB-enriched shell may trigger a new SB in the bulge. In general, the smaller η is, the earlier the reverse shock front moves back to the center.

3.1.3. *Dependence on the gradual feedback*

A reduced Type Ia SN energy input rate (e.g., due to a smaller R_0 and/or E_{SN} than the assumed) has a similar effect as that of a reduced SB feedback on the galactic gas dynamics: the decrease of energy input cannot support a galactic wind or an outflow, and even results in an inflow at later time. We test a model with half of the rate adopted in the reference model, and find that the reverse shock and the cooled SB-enriched dense shell moved back to the center about 2 Gyr ago. The resultant flow has an artificially cold core with a high inner density, similar to the figures shown in Ciotti et al. (1991, fig. 2) and Pellegrini & Ciotti (1998, Fig. 3), which consumes nearly all the energy feedback locally near the bulge center in the 1-D single phase modeling. Such a cold core should undergo additional feedback like nuclear starburst. We do not intend to address such complicated situations here.

A reduction in the mass loss rate has the opposite effect. With the same energy input, but a smaller mass loss rate, the specific heating of stellar ejecta would increase, helping to launch a bulge wind. A reduced mass loss rate would also decrease the diffuse X-ray emission. In reality the mass loss rate is most likely larger than the value calculated from Eq. (8), which is based on a single burst of star formation scenario. The large uncertainty of the mass loss rate comes from the mass loading from heating of cool gas clumps (e.g., the leftover of the SB, cold inflow streams, etc.), in addition to the variation caused by IMF (e.g., a Kroupa IMF gives 12% more mass loss than Salpeter IMF does; see fig. 22 in Maraston 2005). In Model VB we double the stellar mass loss rate given by Eq. (8). In this model the inner bulge wind region has shrunk to a radius less than 20 kpc at $z = 0$ (dotted grey line in Fig. 5). Inside the shocked bulge wind region the density is about twice that of the reference model, and the density profile is leveling off outside. An even larger mass loss rate can quench the inner bulge wind quickly, inducing an inflow by $z = 0$.

The gas dynamics is also affected by how the Type Ia SN rate evolves (e.g, the choice of p if a power law is assumed). The inner bulge wind can be established more easily initially in a model with faster evolutionary trend (i.e, with larger p). To examine this effect we adopt $p = 1.6$ in model VC, and adjust R_0 to ensure that this model has the same total amount of SNe Ia energy input as the reference model. The profiles at $z = 0$ are shown in Fig. 5 (dashed red lines). In this model more SNe Ia explode at early time so that the initial blastwave is stronger and can drive the outermost shock front further away than the reference model does. But at $z = 0$ the resultant bulge wind region is smaller and the temperature is lower because less energy is available to maintain the galactic flow at the late stage. A similar test is done for $p = 1.0$ (Table 2 model VD). Though initially the blastwave is weaker and the outermost shock front has a smaller galactocentric radius, this model maintains a much stronger bulge wind at $z = 0$ because it has a higher Type Ia rate at

the present time.

3.1.4. *Dependence on the treatment of cooled gas*

The effect of the collapsed dense shell on the hot gas flow depends on the coupling of the cooled and hot gases. While the physical processes will be studied in our 2-D modeling (Tang & Wang 2008, in preparation), here we examined the effect in an extreme case by adding a simple “dropout” recipe in our simulation to decouple the cooled gas from the hot gas flow. When a gas pixel cools below the minimum temperature allowed, we dropout 99% of its mass and increase its temperature accordingly to keep the pressure unchanged. Using this recipe, the dropout does not generate numerical perturbation into the simulation and conserves the energy in the flow. Simulations with or without the dropout can thus be used to demonstrate the full range of possible dynamic effect. The dropout in general has little effect on the gas dynamics, if the cooled gas shell is located at a large radius. This is the case for the reference model (Fig. 6). With the dropout, the flow just becomes a little “lighter”. But because the gravitational potential is shallow at the large radius, the effect is small.

On the other hand, if the cold dense shell gets close to or actually falls toward the center, the effect on the gas flow can be substantial. The shell imposes a weight that the enclosed hot gas needs to hold, which can result in increased radiative cooling and eventually quench the bulge outflow. As mentioned in previous, for models with a reduced R_0 or η the dense shell moved back to the center and formed an artificially cold core before $z = 0$. When this weight is removed through the dropout, the bulge outflow becomes faster and the radiative cooling becomes slower. The gas evolution of the Model VE with the “dropout” enabled is shown in Fig. 7. In this model, the stellar ejecta is confined in a region less than 100 kpc, the initial inner bulge wind is quickly quenched and turns into a subsonic outflow. The outflow is stagnated around half of the virial radius (i.e., stagnation is defined as the outflow velocity becomes zero), and an accretion flow is built up near the virial radius. Thus a density enhanced region is formed between half of the virial radius and the virial shock. Effective cooling first occurs in SB-enriched material because it has a relatively high density and low temperature (see Fig. 3 as well). Most of the dropout occurs at radius larger than 100 kpc in this simulation. By dropping out the cooler gas, the galactic flow can stay in a quasi-static state for quite a long time, i.e., as for the specific case (model VE) the density and temperature profiles are hardly changed for half of the Hubble time. The outermost shock front (actually powered by SNe Ia which overtakes the blastwave of SB) is still riding on the turnaround Hubble flow at $z = 0$. Note that a global galactic wind is still maintainable by the gradual stellar feedback if this model starts from a *gas free* initial condition, and the corresponding profiles of density and temperature are shown as the dotted gray lines in Fig. 7.

3.2. Baryonic contents and X-ray Emission

The stellar feedback results in a baryonic mass deficit within the virial radius. The radial variation of the local baryonic fraction (the baryon to total gravitational mass at each galactocentric radius) of the reference model is shown in the left panel of Fig. 8, and the corresponding accumulative baryonic fraction (the total baryonic mass to the total gravitational mass within that radius) is shown in the middle panel. The dash-dot blue line denotes the radial variation at the starburst time t_{sb} . The variation of the local baryonic fraction at this time follows the fluctuation of the simulated dark matter profile given by the 1-D Lagrangian code (see Figure 1). The cumulative fraction shows that the baryonic mass fraction decreases nearly monotonically and reaches the universal value around the virial radius. At $z=0$, the baryon fraction drops down to about 5% near the virial radius and reaches the minimum value at the contact-discontinuity between the materials from the two feedback phases. The baryon fraction then increases outward and finally reaches the universal fraction at the forward blastwave (located at a distance about 6 times the virial radius). This increase is contributed by the SB-enriched material and the shock-compressed IGM. Within the virial radius, the hot gas contribution is negligible, as shown by the dash red line (the inner part has been scaled up by a factor of 10^3 in the plot for easy visualization).

The amount of baryonic mass within the virial radius depends on feedback parameters, such as the strength of the SB and the gradual stellar feedback. The cumulative baryonic mass fraction of Model VA, for example, is shown in the right panel of Figure 8. With the reduced SB efficiency, the baryonic mass fraction at $z = 0$ is higher around the virial radius than that of the reference model. In Table 2 we list the baryonic mass fractions for all the models within one and two virial radii, respectively. For models with strong SB feedback (i.e., Models Ref., VC, and VD), the baryonic fractions within one virial radius are about 5%, and the fractions are even lower within two virial radius, which demonstrates that a large fraction of the baryonic mass is expelled out to a region beyond two virial radius. In Model VE the baryonic fraction is slightly less than the universal value because of its weak stellar feedbacks.

The X-ray luminosities are listed in Table 2 for all the models. We calculate the 0.3-2.0 keV band luminosities within two radii for each model. The luminosities within 2 kpc characterize the diffuse X-ray emission from the inner bulge wind. The X-ray luminosity of the reference model in the inner region is $\sim 2.5 \times 10^{35}$ ergs s^{-1} , and in Model VE the X-ray luminosity is $\sim 4 \times 10^{36}$ ergs s^{-1} . The X-ray luminosities within the virial radius vary dramatically with respect to different models. In the reference model it is only $\sim 4.5 \times 10^{35}$ ergs s^{-1} , whereas in Model VE the luminosity is as high as $\sim 2 \times 10^{39}$ ergs s^{-1} .

4. Discussion

We now discuss the implications of the above results in connection to the issues mentioned in §1 and the additional work that is needed to further the study of the feedback scenario proposed

here.

4.1. The Over-cooling Problem

Our simulations demonstrate that the total accreted baryonic mass (cold phase plus hot phase) can be largely reduced when the stellar feedback is properly introduced. Except Model VE, the baryonic mass fractions of other models are only about 5% within virial radius, consistent with an inferred low baryonic fraction in the Milky Way (roughly about 6%, e.g., McGaugh 2007; Fukugita & Peebles 2006; Sommer-Larsen 2006; Maller & Bullock 2004). In our reference model, the radiative cooling after the SB is small because of the low density and high temperature of the halo gas. Here the feedback is treated self-consistently for both the internal heating of the intrahalo gas (within a galaxy’s virial radius) and the external “pre-heating” of the surrounding IGM. The rarification of the pre-heated IGM substantially reduces and even reverses the accretion. The degree of the rarification can be characterized by the baryonic deficit around a galaxy (e.g., Fig. 8).

The amount of cooling by the gaseous halo at the present can, in principle, allow for placing constraints on η . For a too small η , the gas would not be sufficiently pre-heated to reduce the accretion into the halo, and the baryonic mass fraction would be much closer to the cosmic universal value, as shown in Model VE. The total cooling rate¹ of the gas around the reference galaxy is only a few of 10^{37} ergs s^{−1}, the bulk of which arises from the accumulated reverse-shocked bulge wind material, located outside of the virial radius (see Fig. 9 left panel). For the model with a lower η value, the cooling would be more efficient and occurs in regions closer to the bulge. In general, no over-cooling problem occurs in our model of galaxy evolution with the proper stellar feedback.

4.2. The Missing Stellar Feedback Problem

The conventional models interpret that the missing energy is gone with bulge outflows (e.g., Mathew & Baker 1971; Lowenstein & Mathews 1987; Ciotti et al. 1991). Probably the most thorough study of hot gas outflows around ellipticals is by Ciotti et al. (1991). Under the assumption of a static galactic halo with a *gas free* initial condition, presumedly generated by an initial SB, their 1-D model galaxies evolve through up to three consecutive evolutionary states: an initial wind, a transition to subsonic outflow, and a final inflow phase. X-ray faint ellipticals are suggested to be in their wind phase, and brightest ellipticals should mostly be in the inflow regime. The subsonic outflow is shown to be unstable and short-lived.

Our simulations have shown that the SB feedback is able to produce a low-density environment

¹The bolometric luminosity is calculated based on cooling function with solar abundance (Sutherland & Dopita 1993), and less than 10% is radiated in 0.3-2.0 keV band.

near the galactic bulge, which is similar to the “gas-free” condition assumed in Ciotti et al. (1991). But, different from what the early model predicted, the stellar bulge feedback material does not leave the galaxy freely. Much of the feedback energy may be thermalized well inside the virial radius, forming a hot gaseous halo. The bulge wind solution applies only within the reverse shock front, shown by dot-dashed blue lines in Figure 4, for example. When the reverse shock moves inward, the wind becomes less and less developed and may eventually turn into a global subsonic outflow. We find that this subsonic outflow is stable, in contrast to the result of Ciotti et al. (1991). The unstable and short life of the subsonic outflow in their model is apparently caused by the use of the “outflow” outer boundary condition, which is generally not consistent with the changing properties of the galaxy and its environment. The “outflow” boundary condition has no effect on the internal flow, as long as the outflow is supersonic. But if subsonic, however, the outflow tends to be suppressed by the artificial force inserted by the leveled off pressure at the boundary; while an inflow would be amplified, which quickly quenches the inner bulge wind/outflow. In our model, no boundary condition needs to be assumed for the bulge wind/outflow, because it occurs well inside the spatial range of the simulations.

The stability of the subsonic outflow state has strong implications for understanding the large scattering of L_X/L_B of galactic bulges. The distribution of the hot gas in the state depends not only on the feedback in the bulge, but also on the condition in outer regions of the galactic halo, which is a manifestation of the large-scale environment and formation history of a galaxy. This dependence can create a large diversity in the X-ray luminosities of such galaxies.

For the bulge outflow to be the solution of the missing feedback problem, a sufficient mechanical energy output from both the SB and Type Ia SNe is needed. A weak SB (e.g., a too small η value) would not create an environment with a low enough density for a lasting galactic bulge outflow. Even with a large SB feedback, a too low SNe Ia rate would lead to the blowout gas being re-accreted into the halo. Once an inflow is developed near the bulge, the feedback from SNe Ia would be consumed locally, producing a luminosity comparable to the input, which is disfavored by current observations.

While our 1-D model may provide a reasonably good characterization of the large-scale impact of the stellar bulge feedback, the bulge wind/outflow is inefficient in producing diffuse X-ray emission. In particular, we find that the X-ray luminosity from the 1-D wind/outflow is considerably lower than what is observed from galactic bulges. Observationally the reported “diffuse” X-ray emission of our Galactic bulge and the one in M31 are about 10^{38} ergs s $^{-1}$ (Shirey et al. 2001; Takahashi et al. 2004; Li & Wang 2007). For all the models, the X-ray emissions from the inner region are no more than a few of 10^{36} ergs s $^{-1}$. Although $\sim 60\%$ of the energy is radiated within half of the virial radius in Model VE, its X-ray emission near the bulge region is only a few times 10^{36} ergs s $^{-1}$. Note that in Model VE about 40% of the total energy input is used to remove the stellar mass ejecta out of the gravitational well at $z = 0$ and a less fraction is required at early time. It is also worth pointing out that the diffuse X-ray surface brightness of bulge winds is in general steeper than that of stellar mass/light as demonstrated in Fig. 9 right panel (see also Ciotti et al.

1991, fig. 6). Only the model VE, in which the gas flow is now in a subsonic outflow state, has a flatter surface brightness, consistent with observations of X-ray-faint early-type galaxies (e.g., O’Sullivan & Ponman 2004).

The X-ray deficit of the bulge winds could be caused by our simplified 1-D model. A careful analysis of the X-ray emission from the M31 bulge indicates the presence of a truly diffuse component with a 0.5-2 keV luminosity of $\sim 2 \times 10^{38}$ ergs s $^{-1}$ (Li & Wang 2007). However, this component has a substantially lower temperature (~ 0.4 keV) and a bipolar morphology in and around the bulge. These facts indicate that much of this soft X-ray component arises from the interaction of hot gas with cool gas and that the 1-D approximation is too simplistic, at least in the immediate vicinity of the bulge region, which may be expected because of the presence of cool gas in the galactic disk. A detailed study shows that this interaction may indeed be important, especially for the calculation of X-ray emission, which is sensitive to presence of density structures. We are carrying out detailed 2-D and 3-D simulations of the M31 bulge region and comparisons with corresponding X-ray observations. The results will be reported in separate papers.

4.3. Additional Remarks and Caveats

Stellar feedback is an important process in the co-evolution of galactic bulge and host galaxy. The two-stage stellar feedback model we introduced in this paper naturally sets up the stellar feedback from the galactic bulges in the context of the assembly history of the host galaxy/halo. In the first stage, the violent galaxy mergers in the fast-assembly regime trigger a starburst which instantaneously releases feedback energy through core-collapsed explosions to expel a large fraction of the halo gas; in the second stage, the old stellar population in the bulge provides a long-lasting feedback via Type Ia SNe to keep the gaseous halo hot. In this model, the SB feedback and the gradual feedback are roughly synchronized with the early violent merger stage and the later gentle accretion stage of the host galaxy, which is a generic picture of galaxy formation in the CDM model. A similar co-evolution scenario has been proposed for AGN feedback (Croton et al. 2006). In their scenario, a central massive black hole builds up its mass during galaxy mergers, and the black hole appears as a “quasar”; when a static hot halo has formed in the latter time, the cooling halo gas fuels the central massive black hole to make it active in a so-called low-energy radio mode. Although our stellar feedback model and the AGN feedback scenario are aimed at two different processes in galaxy formation, they share some common features. Firstly, the feedback processes happen in two distinct regimes, an early energetic but short-term blow-out and a late low-energy level but long-lasting heating. Secondly, the feedback and the galaxy formation are modeled in a co-evolving fashion. However, our stellar feedback model is proposed for the MW-sized galaxies, whereas the AGN scenario is proposed to work for more massive galaxies, which contribute to the bright end of the galaxy luminosity function.

Clearly, the model adopted here is idealized. Substantial deviation from our model assumption is possible and may significantly alter our results. Here we discuss briefly some of these possibilities.

How galactic stellar bulges really form remains a question of debate. It is likely that there are multiple formation paths. A popular paradigm is the formation through galaxy merges (instead of a monolithic collapse), which typically happen at high redshifts. In fact, our halo growth model is based on the average mass accretion history from N -body simulations (e.g., Wechsler et al. 2002; Zhao et al. 2003a,b). After the last major merger, a bulge evolves nearly passively, except for some minor mergers. If the bulk of bulge stars are formed in a SB during the last major merge, our model still applies. However, if the bulge formed primarily from pre-existing stars by mergers (the so-called dry mergers), a direct application of our model would not be appropriate.

Much of existing work on stellar feedback is focused on whether or not a SB could drive a galactic superwind. Silk (2003) has argued that outflows can escape from massive galaxies provided that the porosity of the ISM $Q \sim 1$, probably with the aid of supernovae, a top-heavy IMF, and/or AGN heating. In the model we have examined here, the question whether a SB-driven outflow can escape or not is not particularly relevant, because the galaxy is evolving and the galaxy environment is not gas-free. More relevant is the cooling time scale of the SB-heated material near the galactic bulge. This cooling time depends on the detailed physical processes involved in the interplay between massive stars and the ISM, which our simple model does not take into account. Depending largely on the assumed value of η , the SB-heated material may have already fallen back to the center or is still hanging in regions outside the galactic virial radius. Our choice of the initial condition of the SB material (the distribution scale) guarantee that the cooling time-scale is long enough for the Type Ia SN-driven wind to develop an outflow. It is the rarification of the halo gas by SB feedback that helps the Type Ia SN-driven outflow to gently blow out the accreted material and replenish the ISM with mass from evolving stars.

We have considered galaxies in “isolation”. This approximation may be reasonable for field galaxies, especially at high redshifts. But as shown in our simulations, the stellar feedback may have significant effects on the IGM on scales considerably larger than the virial radius of individual galaxies. Such impact may be sufficient to influence the IGM environments of member galaxies in groups. For example, much of the gas in the Local Group, which contains two MW-like galaxies with a substantial stellar bulge component, may have been heated to a temperature of $\sim 10^7$ K (e.g., Fig. 3). Such hot gas with too low a density to be easily detected is consistent with the exiting observations of large-scale gaseous halos. Ironically, the stellar energy feedback in groups containing galaxies with more massive halos (e.g., giant ellipticals) may have relatively minor effects, compared to the gravitational heating.

In our numerical model, mass accretion is assumed to be smooth. In reality, however, the accretion is more complicated. N -body simulations of cosmic structure formation have shown that dark matter halos acquire their masses mainly through lumpy mergers rather than smooth accretion. The SPH galaxy formation simulations have further indicated that the gas accretion comes from both a smooth “hot” mode and a clumpy “cold” mode (Kereš et al. 2005). As discussed in Voit et al. (2003), lumpy accretions may give rise to higher entropy in the IGM than smoothed accretion, and hence may result in less cooling. In addition, since denser clumps are difficult to

be heated when going through the accretion shock (e.g. Voit et al. 2003; Poole et al. 2006), the gas accretion in different modes gives rise of a multi-phase medium. The multi-phase medium may largely alter the assembly history of the central galaxy, and hence changes the evolution of the stellar feedback and the thermal properties of the halo gas (Mo & Miralda-Escude 1996; Maller & Bullock 2004; Kaufmann et al 2006). The details about such a multi-phase medium are still poorly understood. The expectation is that the multi-phase medium may increase the gas accretion rate onto the central galaxy, hence boosting the predicted X-ray luminosity. The cold accretion may also be responsible to some of the observed HVCs around our the Galaxy (e.g., Sembach et al. 2003), in addition to those that might be produced by the cooled feedback material discussed in §3.1.4.

5. Summary

We have examined the potential impacts of the galactic stellar bulge feedback on the hot gaseous structure and evolution around galaxies. We have focused on early-type spirals such as the MW, M31 and ellipticals with low L_X/L_B ratios, indicating ongoing mass and energy outflows. The feedback in such a galaxy is approximately divided into two phases: 1) a SB-induced blastwave from the formation of the bulge and 2) a gradual energy and mass injection from bulge stars. Our 1-D model deals with the feedback in the galaxy evolution context, approximately accounting for the dark matter accretion history. We have carried out various simulations with this model to demonstrate the impacts and their dependences on key assumptions and parameters used. Our major results and conclusions are as follows:

- The blastwave initiated during the SB and maintained by subsequent Type Ia SNe in a galactic bulge may heat the IGM beyond the virial radius, which may stop further gas accretion. The heated gas expands and produces a baryon deficit around the galaxy.
- The high temperature and low density of the remaining gas in the galactic halo produces little X-ray emission, consistent with existing observations. Thus the inclusion of both the SB and Type Ia SN feedbacks may provide a solution to the theoretic “over-cooling” problem.
- With the low-density galactic halo environment, the gradual stellar feedback, powered by Type Ia SNe alone, can form a galactic bulge wind, especially when the bulge is young. Much of the tenuous hot halo is occupied by the thermalized bulge wind material. The bulge wind region shrinks and likely turns into a subsonic outflow as the SN rate decreases. This wind/outflow naturally explains the *missing stellar feedback* problem of galactic bulges.
- We find that a subsonic outflow from a galactic bulge can be a long-lasting state, the properties of which depend sensitively on the environment and formation history of the galaxy. This dependency may account for the large dispersion in the X-ray luminosities of galaxies with similar L_B .

Acknowledgments

The software used in this work was in part developed by the DOE-supported ASC / Alliance Center for Astrophysical Thermonuclear Flashes at the University of Chicago. This project is supported by NASA through grant SAO TM7-8005X and NNG07AH28G. HJM would like to acknowledge the support of NSF AST-0607535, NASA AISR-126270 and NSF IIS-0611948.

REFERENCES

- Arthur N, Cox, 1999, *Allen’s Astrophysical Quantities*, fourth edition
Aubourg, E., Tojeiro, R., Jimenez, R., et al. 2007, *astroph/0707.1328v2*
Blumenthal G. R., Faber S. M., Flores R., Primack J. R., 1986, *ApJ*, 301, 27
Bullock J. S., Kolatt T. S., Sigad Y., Somerville R. S., Kravtsov A. V., Klypin A. A., Primack J. R., Dekel A., 2001, *MNRAS*, 321, 559
Bond J. R., Cole S., Efstathiou G., Kaiser N., 1991, *ApJ*, 379, 440
Brighenti F., Mathews W. G., 1999, *ApJ*, 512, 65
Bryan G. L., Norman M. L., 1998, *ApJ*, 495, 80
Cappellaro E., Evans R., Turatto M., 1999, *A&A*, 351, 459
Ciotti L., D’Ercole A., Pellegrini S., Renzini A., 1991, *ApJ*, 376, 380
Choi J., Lu Y., Mo H. J., Weinberg M. D., 2006, *MNRAS*, 372, 1869
Croton D. J., et al., 2006, *MNRAS*, 365, 11
Davé, R., Oppenheimer, B. D., 2007, *MNRAS*, 374, 427
David L. P., Forman W., Jones C., 1990, *ApJ*, 359, 29
David L. P., Jones C., Forman W., Vargas I. M., Nulsen P., 2006, *ApJ*, 653, 207
Fryxell B., et al., 2000, *ApJS*, 131, 273
Fujita, A., Mac Low, M. M., Ferrara, A., & Meiksin, A. 2004, *ApJ*, 613, 159
Fujita A., Ma L. M., Ferrara A., Meiksin A., 2004, *ApJ*, 613, 159
Gnedin N. Y., 2000, *ApJ*, 542, 535
Hoeft M., Yepes G., Gottlöber S., Springel V., 2006, *MNRAS*, 371, 401
Greggio L., 2005, *A&A*, 441, 1055
Hernquist L., 1990, *ApJ*, 356, 359
Jing Y. P., Suto Y., 2000, *ApJ*, 529, L69
Kaufmann T., Mayer L., Wadsley J., Stadel J., Moore B., 2006, *MNRAS*, 370, 1612
Kereš D., Katz N., Weinberg D. H., Dave R., 2005, *MNRAS*, 363, 2
Kroupa P., 2001, *MNRAS*, 322, 231
Li Z., Wang Q. D., Irwin J. A., Chaves T., 2006, *MNRAS*, 371, 147
Li Z., Wang Q. D., Hameed S., 2007, *MNRAS*, 376, 960
Li Z., Wang Q. D., 2007, *ApJ*, 668, L39
Loewenstein M., Mathews W. G., 1987, *ApJ*, 319, 614
Lu Y., Mo H. J., Katz N., Weinberg M. D., 2006, *MNRAS*, 368, 1931

- Lu Y., Mo H. J., 2007, *MNRAS*, 377, 617
- Ma L. M., Ferrara A., 1999, *ApJ*, 513, 142
- Maller A. H., Bullock J. S., 2004, *MNRAS*, 355, 694
- Mannucci F., Dell V. M., Panagia N., 2006, *MNRAS*, 370, 773
- Maraston, C. 1998, *MNRAS*, 300, 872
- Maraston C., 1998, *MNRAS*, 300, 872
- Mathews W. G., Baker J. C., 1971, *ApJ*, 170, 241
- McGaugh S. S., 2007, *IAUS*, 244, 136
- Miller G. E., Scalo J. M., 1979, *ApJS*, 41, 513
- Mo H. J., Mao S., 2002, *MNRAS*, 333, 768
- Mo H. J., Mao S., 2004, *MNRAS*, 353, 829
- Mo H. J., Miralda-Escude J., 1996, *ApJ*, 469, 589
- Mo H. J., Yang X., van den Bosch, F. C., Katz N., 2005, *MNRAS*, 363, 1155
- Moore B., Governato F., Quinn T., Stadel J., Lake G., 1998, *ApJ*, 499, L5
- Navarro J. F., Frenk C. S., White S. D. M., 1996, *ApJ*, 462, 563
- O’Sullivan E., Ponman T. J., 2004, *MNRAS*, 349, 535
- Pellegrini S., Ciotti L., 1998, *A&A*, 333, 433
- Poole G. B., Fardal M. A., Babul A., McCarthy I. G., Quinn T., Wadsley J., 2006, *MNRAS*, 373, 881
- Press W. H., Schechter P., 1974, *ApJ*, 187, 425
- Quinn T., Katz N., Efsthathiou G., 1996, *MNRAS*, 278, L49
- Revnivtsev M., Sazonov S., Gilfanov M., Churazov E., Sunyaev R., 2006, *A&A*, 452, 169
- Sembach K. R., et al., 2003, *ApJS*, 146, 165
- Sheth R. K., Mo H. J., Tormen G., 2001, *MNRAS*, 323, 1
- Shirey R., et al., 2001, *A&A*, 365, L195
- Silk J., 2003, *MNRAS*, 343, 249
- Sommer-Larsen J., 2006, *ApJ*, 644, L1
- Strickland D. K., Stevens I. R., 2000, *MNRAS*, 314, 511
- Sutherland R. S., Dopita M. A., 1993, *ApJS*, 88, 253
- Tang S., Wang Q. D., 2005, *ApJ*, 628, 205
- Takahashi H., Okada Y., Kokubun M., Makishima K., 2004, *ApJ*, 615, 242
- Toft S., Rasmussen J., Sommer-Larsen J., Pedersen K., 2002, *MNRAS*, 335, 799
- Voit G. M., Balogh M. L., Bower R. G., Lacey C. G., Bryan G. L., 2003, *ApJ*, 593, 272
- Wechsler R. H., Bullock J. S., Primack J. R., Kravtsov A. V., Dekel A., 2002, *ApJ*, 568, 52
- White S. D. M., Frenk C. S., 1991, *ApJ*, 379, 52
- White S. D. M., Rees M. J., 1978, *MNRAS*, 183, 341
- White R. E. I., Chevalier R. A., 1983, *ApJ*, 275, 69
- Wyithe J. S. B., Loeb A., 2003, *ApJ*, 595, 614
- Zhao D. H., Mo H. J., Jing Y. P., Borner G., 2003a, *MNRAS*, 339, 12
- Zhao D. H., Jing Y. P., Mo H. J., Borner G., 2003, *ApJ*, 597, L9

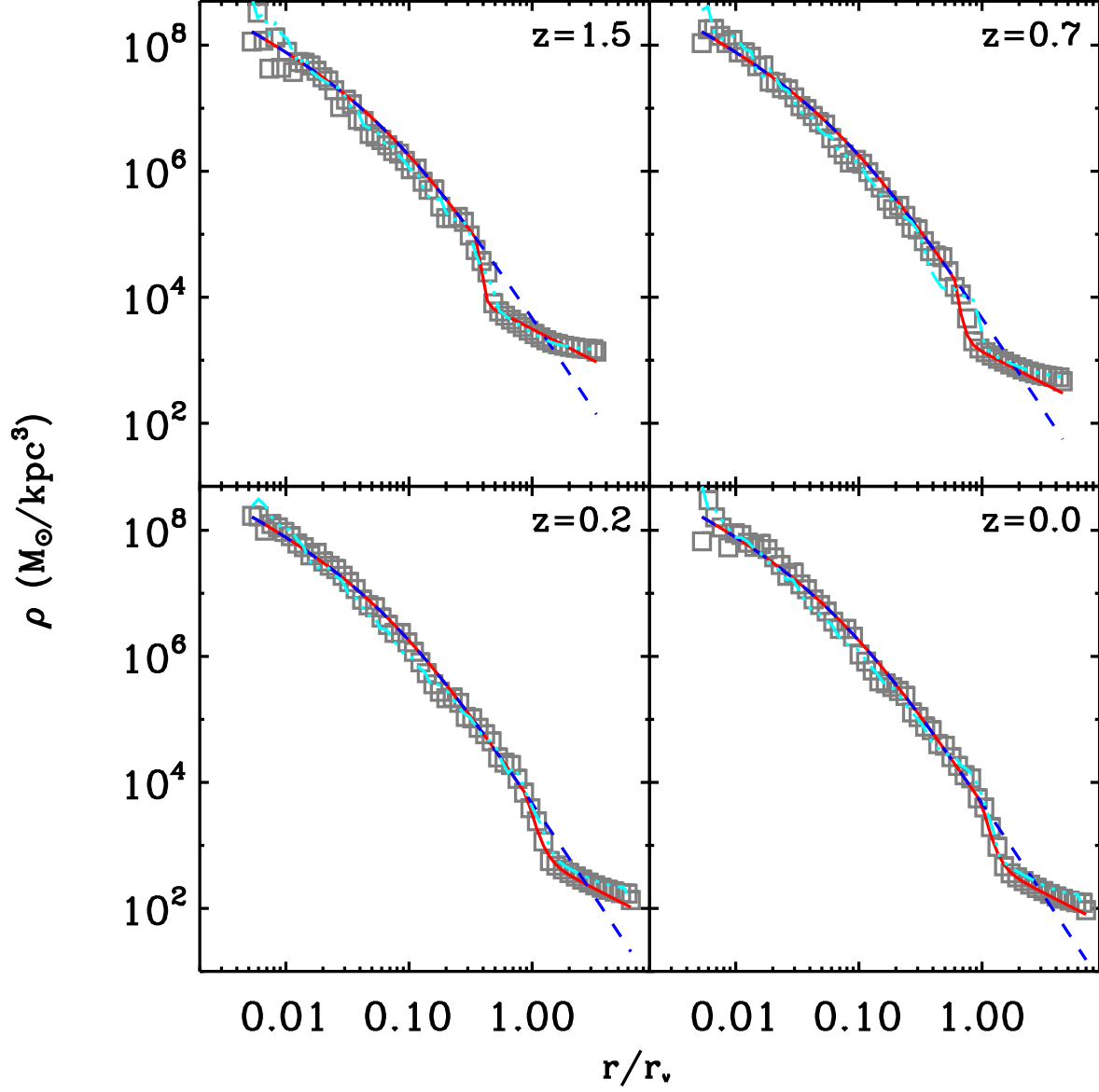


Fig. 1.— Dark matter density profiles of a galaxy of $10^{12} M_\odot$ at $z = 0$ at four representative redshifts: Simulation without stellar feedback (grey squares); NFW profile at $z = 0$ (dashed blue lines); the fitting formula (solid red lines); Simulation including stellar feedback (§2.2) (three-dot-dashed cyan lines).

Table 2. Models of stellar feedback

| Model | R_0 (SNU) | η | p | $^a L_X$ ($10^{36} \text{ergs s}^{-1}$) | | f_b | |
|-----------------|-------------------|--------|-----|---|---------------------------|---------------------------|----------------------------|
| | | | | $(r \leq 2 \text{kpc})$ | $(r \leq r_{\text{vir}})$ | $(r \leq r_{\text{vir}})$ | $(r \leq 2r_{\text{vir}})$ |
| Ref. | 0.12 | 0.5 | 1.4 | 0.25 | 0.45 | 0.045 | 0.040 |
| VA | 0.12 | 0.25 | 1.4 | 0.25 | 18.6 | 0.047 | 0.111 |
| VB ^b | 0.12 | 0.5 | 1.4 | 5.7 | 50.0 | 0.047 | 0.082 |
| VC | 0.06 ^c | 0.5 | 1.6 | 1.2 | 2.8 | 0.046 | 0.041 |
| VD | 0.35 ^c | 0.5 | 1.0 | 0.038 | 0.064 | 0.045 | 0.039 |
| VE ^d | 0.06 | 0.25 | 1.4 | 3.8 | 1673 | 0.163 | 0.168 |

^a L_X is calculated in the 0.3-2.0 keV band, assuming solar abundance. r is the galactocenter radius in units of kpc.

^bthe mass loss rate determined by Eq. (8) is doubled.

^c R_0 is normalized to give the same total energy input as the reference model.

^dThe “dropout” recipe is applied (§3.1.4).

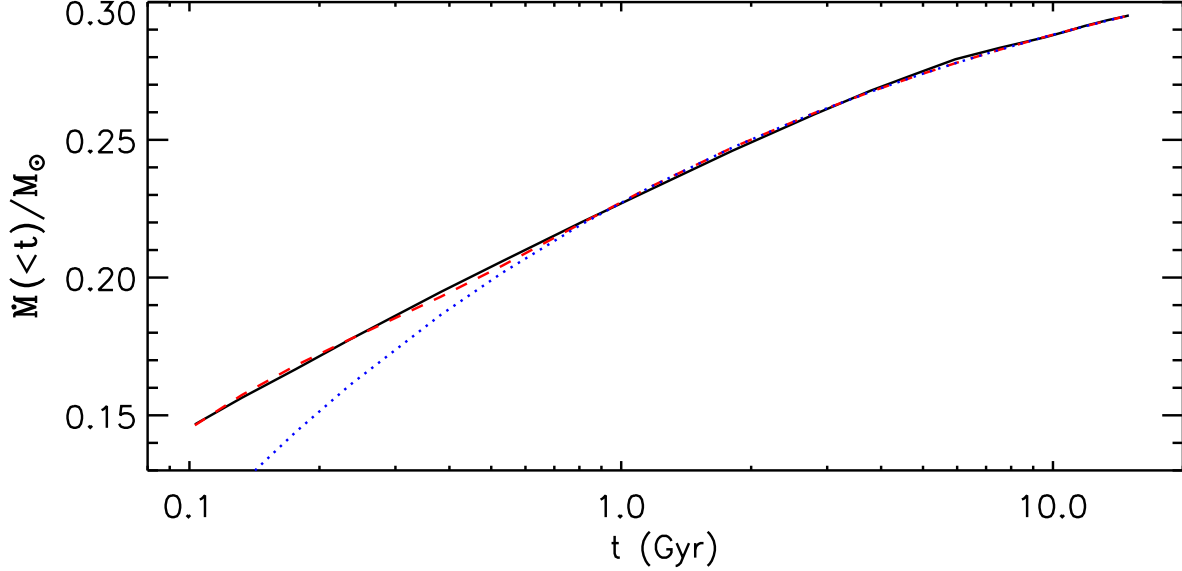


Fig. 2.— The cumulative stellar mass loss of a stellar population (normalized to one M_\odot with the Salpeter IMF) as a function of its age. The solid black line denotes the data taken from Maraston (2005) Figure 22.; the dashed red line is the fitting; the dotted blue line is the component with the same power index as used in Ciotti (1991).

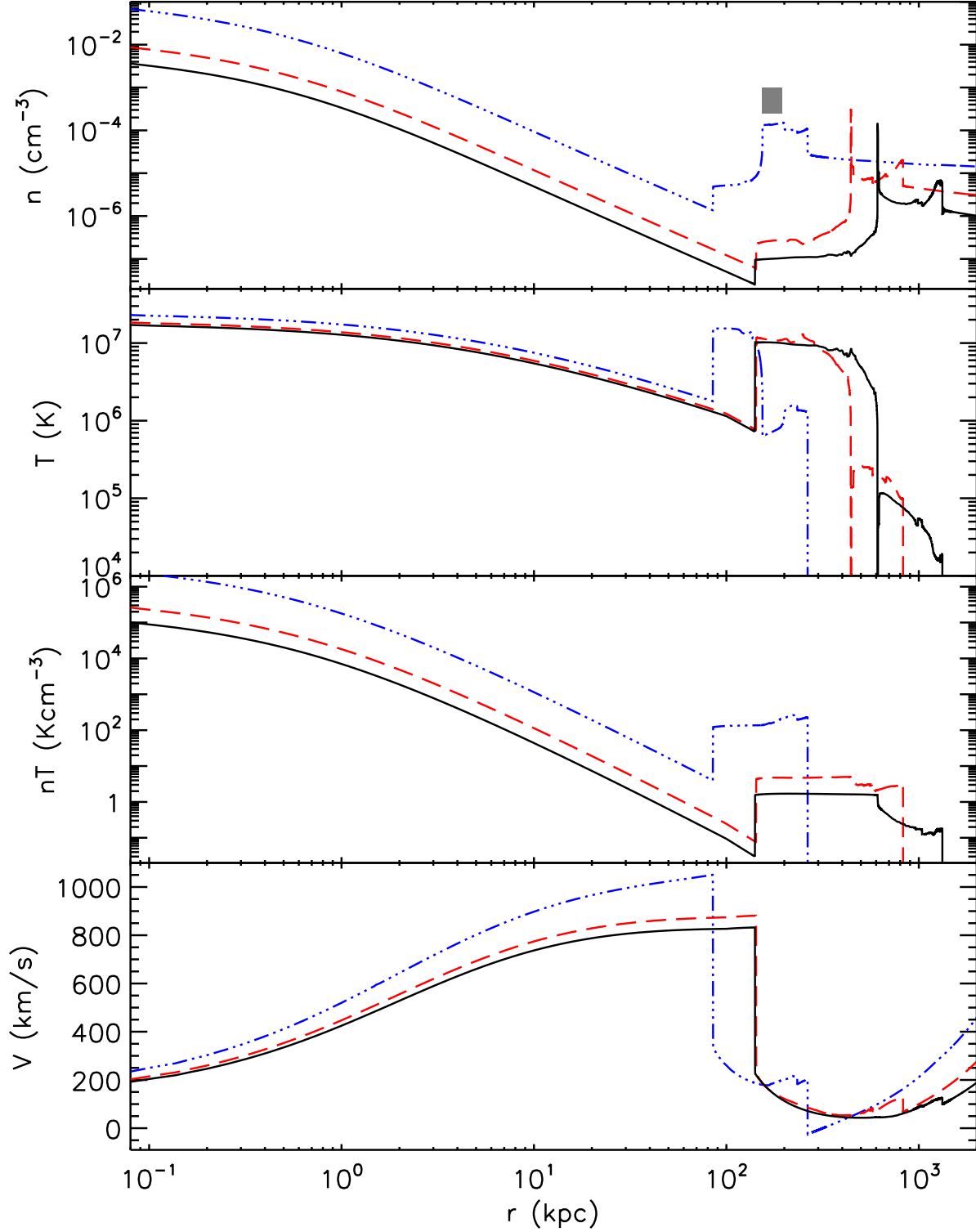


Fig. 3.— Radial profiles of density, temperature, pressure, and velocity of the gas around the simulated reference galaxy at three representative redshifts: $z=1.4$ (dot-dashed blue lines), 0.5 (long-dashed red), and 0.0 (solid black). The filled gray region in the top panel marks the radial range of the SB-enriched material at $z=1.4$. In the lower z profiles, this range has collapsed and is seen as the narrow spikes.

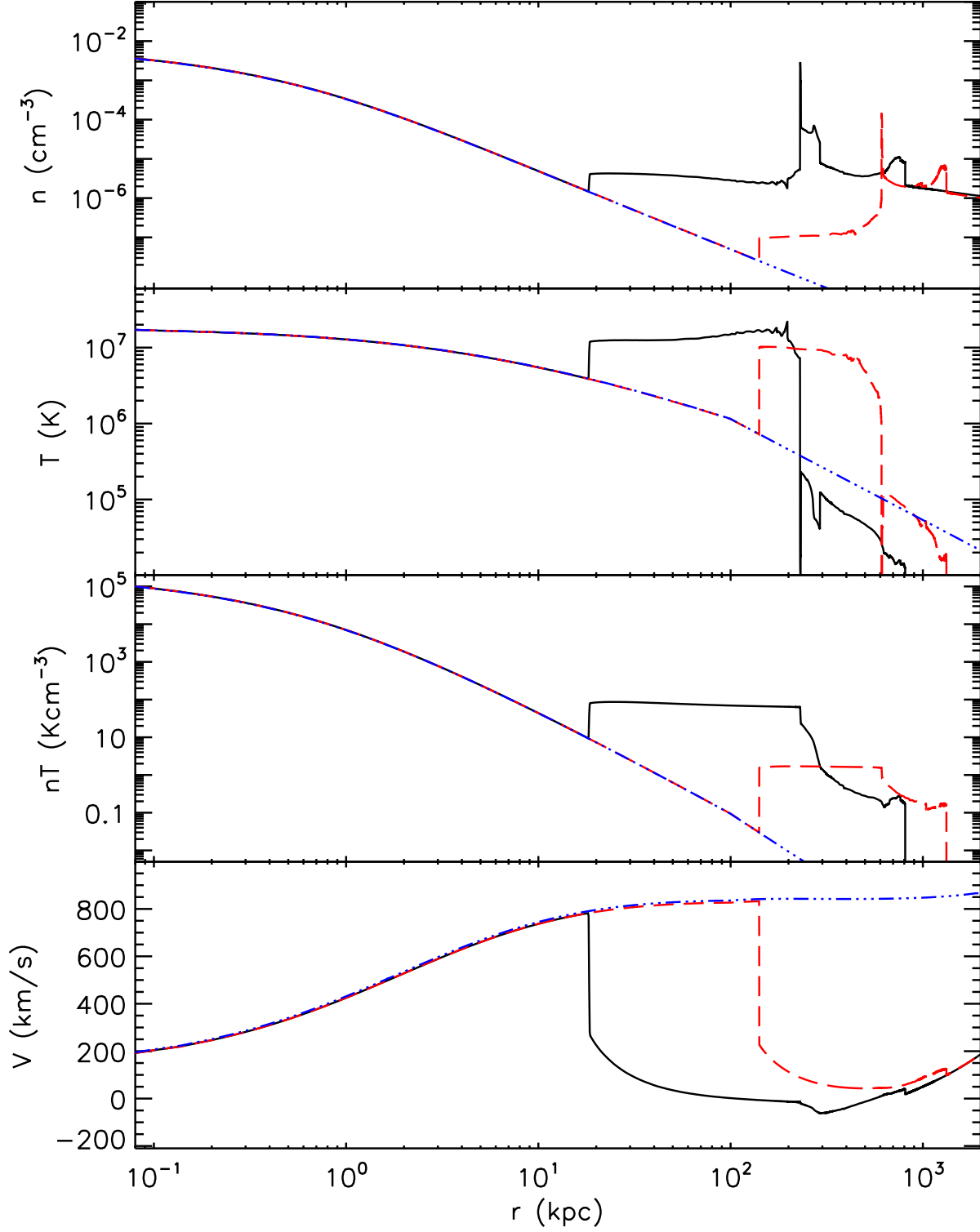


Fig. 4.— Radial profiles at $z=0$ for three models: the reference model (long-dash red lines); Model VA (solid black lines); and a model started with the *gas free* initial condition (three-dot-dashed blue lines).

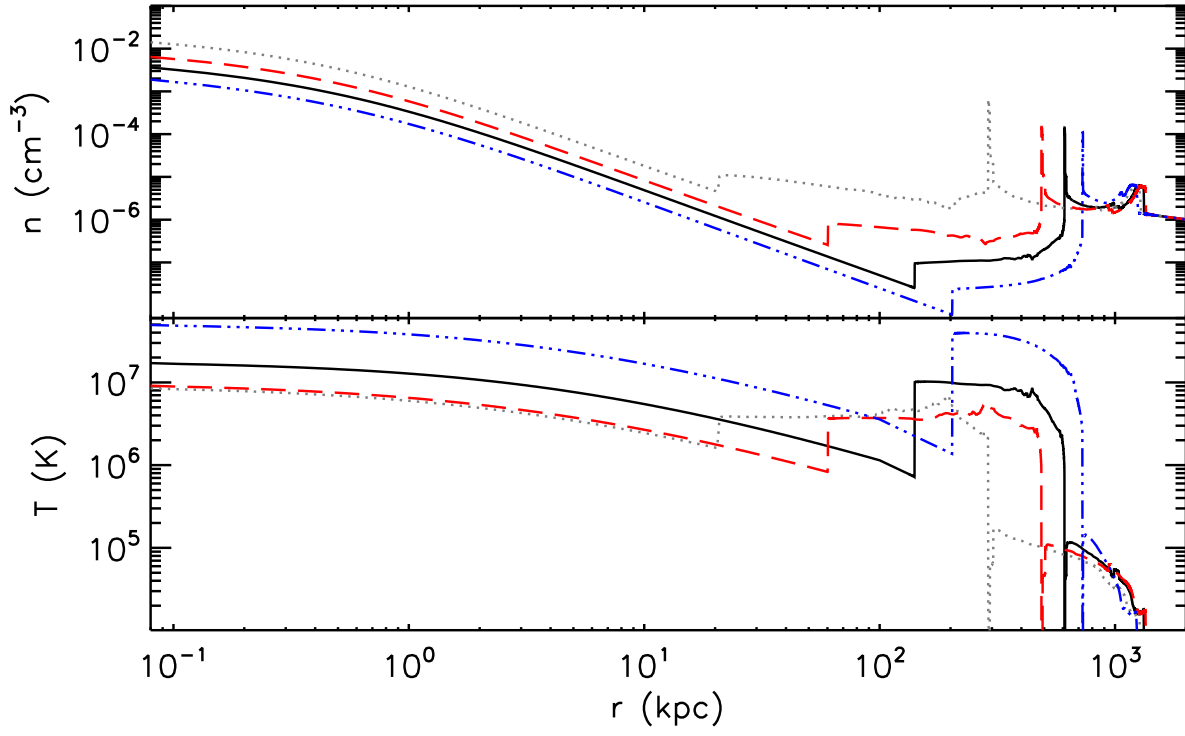


Fig. 5.— Comparison of the radial density and temperature profiles inferred from the models with various gradual feedback parameters at $z = 0$: the reference model (solid black lines), model VB (dotted grey lines), model VC (dashed red lines), model VD (three-dot-dashed blue lines).

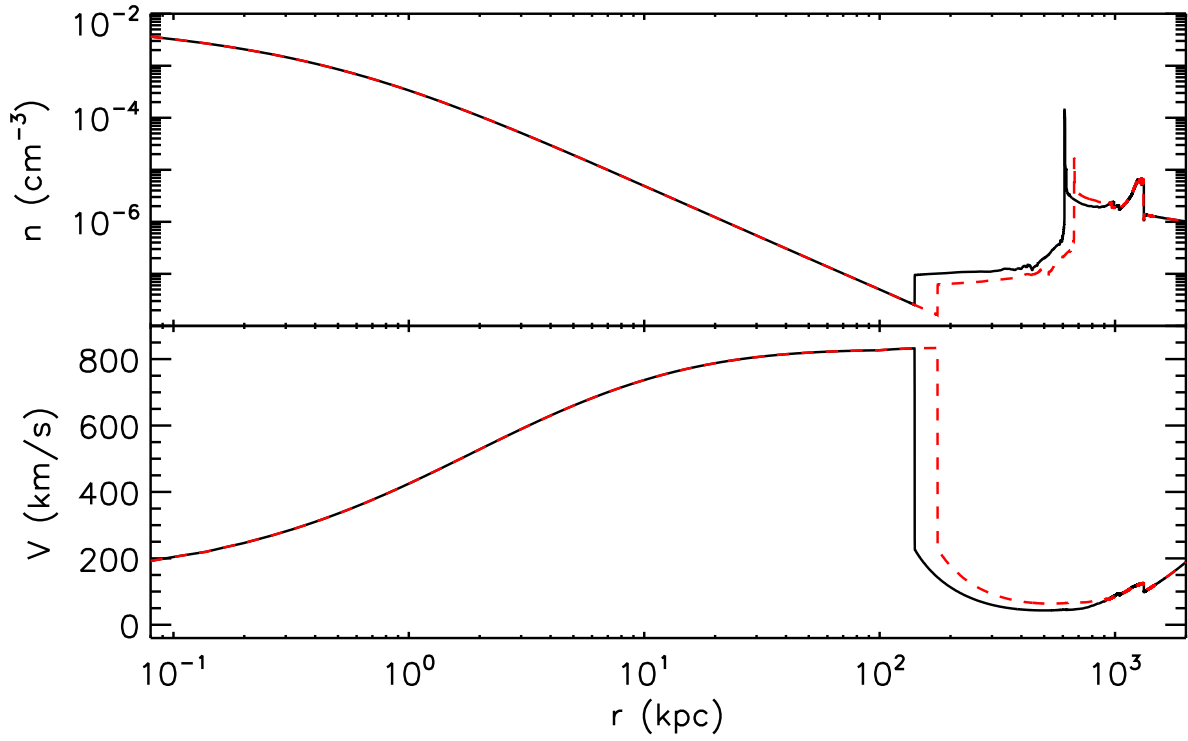


Fig. 6.— Demonstration of the “dropout” effect on the reference model at $z=0$: the reference model (solid black lines), the reference model with the “dropout” included (dashed red lines).

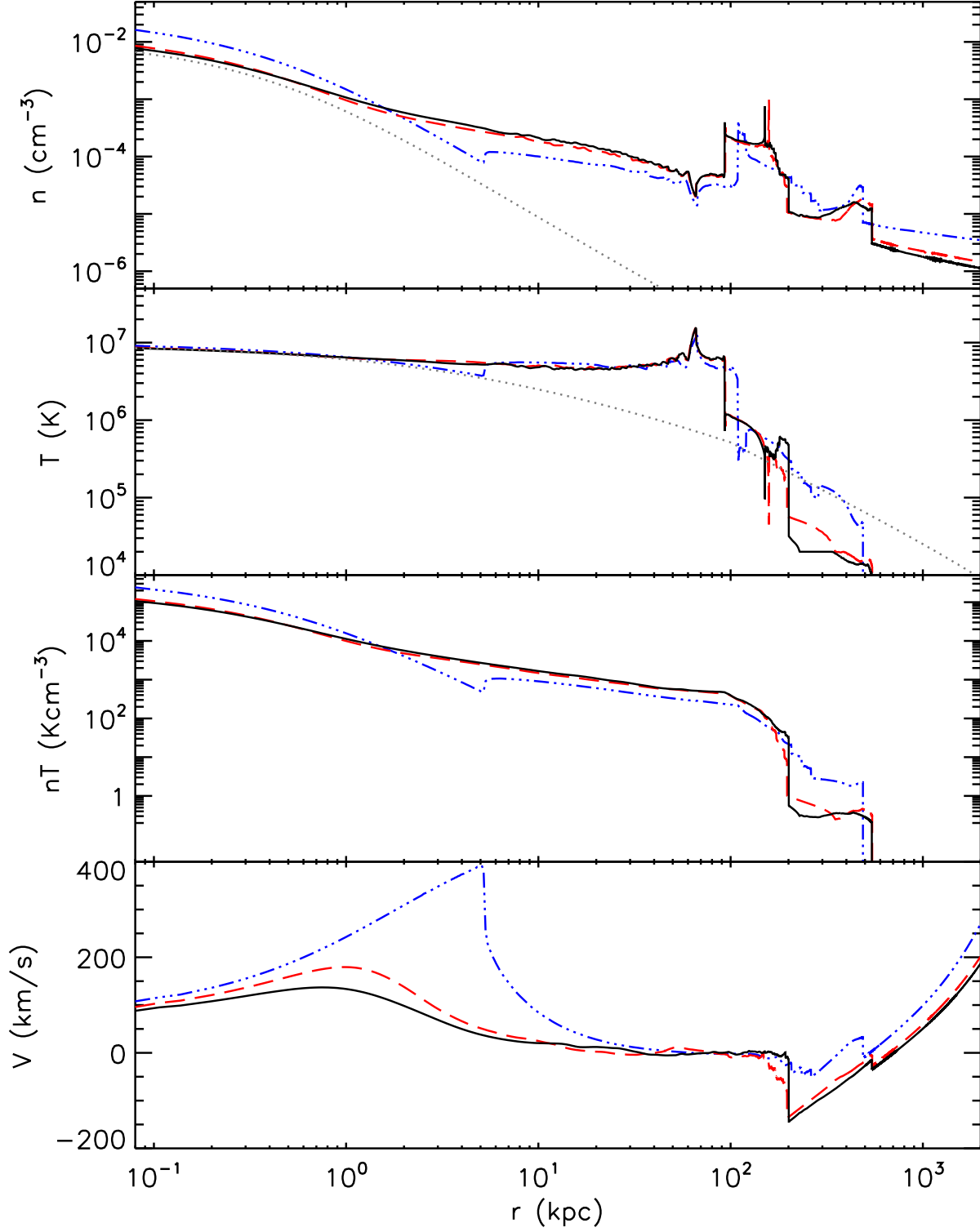


Fig. 7.— Radial profiles of Model VE (with the “dropout” enabled) at three redshifts: $z=0.5$ (three-dot-dashed blue line), $z=0.1$ (dashed red lines), and $z=0.0$ (solid black lines). The dotted grey lines in the top two panels denote the corresponding profiles if model VE starts from a gas free condition.

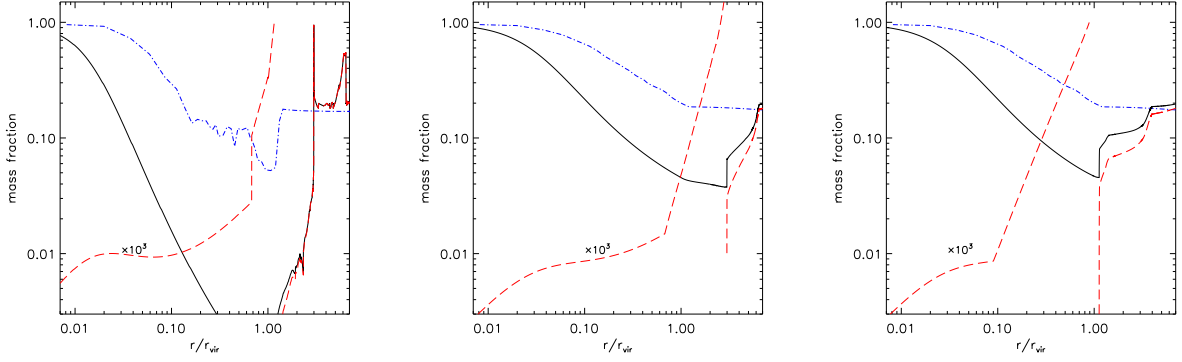


Fig. 8.— The local baryonic fraction as a function of the dimensionless galactocentric radius in the unit of virial radius for the reference model (*left panel*); the accumulated baryonic fraction as a function of the radius for the reference model (*middle panel*) and model VA (Table 2, *right panel*). The dot-dashed blue line is for the total baryonic mass fraction at the starburst time t_{sb} . The solid black line is for the total baryonic mass fraction at $z=0$. Dashed red line denotes the contribution of the hot gas, with the inner part increased by a factor of 10^3 for ease visualization. The fractions reach to the universal value $f_b=0.17$ near the forward shock front located at a few times of the virial radius.

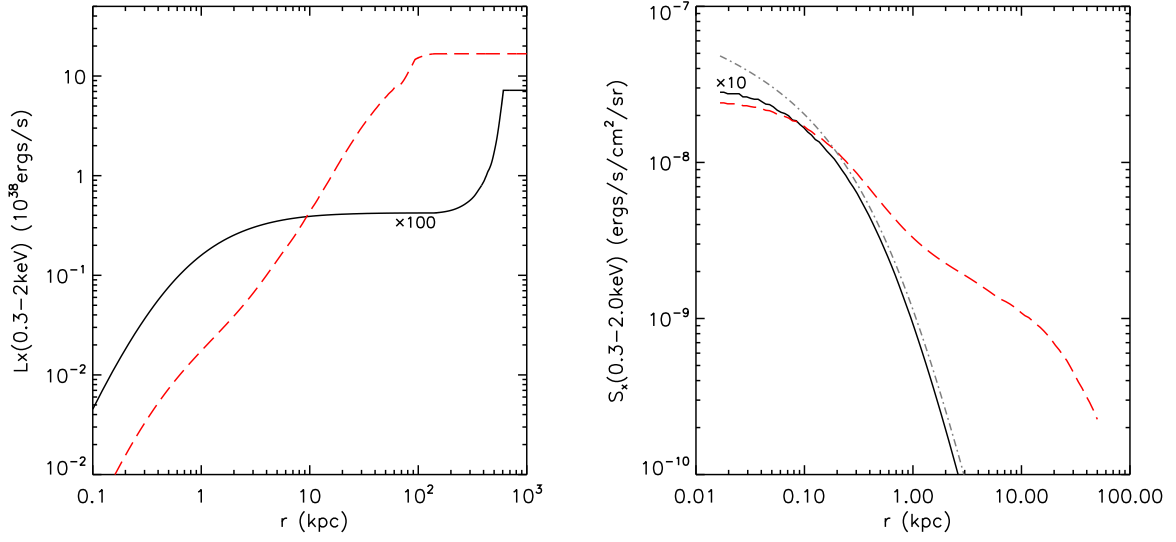


Fig. 9.— *Left Panel:* Cumulative X-ray luminosities as functions of galactocentric radius in the 0.3-2.0 keV band for the reference model (solid black line) and the model VE (solid black line). *Right panel:* The corresponding surface brightness of the X-ray emission, the dot-dashed gray line denotes the stellar surface brightness with an arbitrary normalization. The values of the reference model are multiplied by the marked factor for easy visualization.